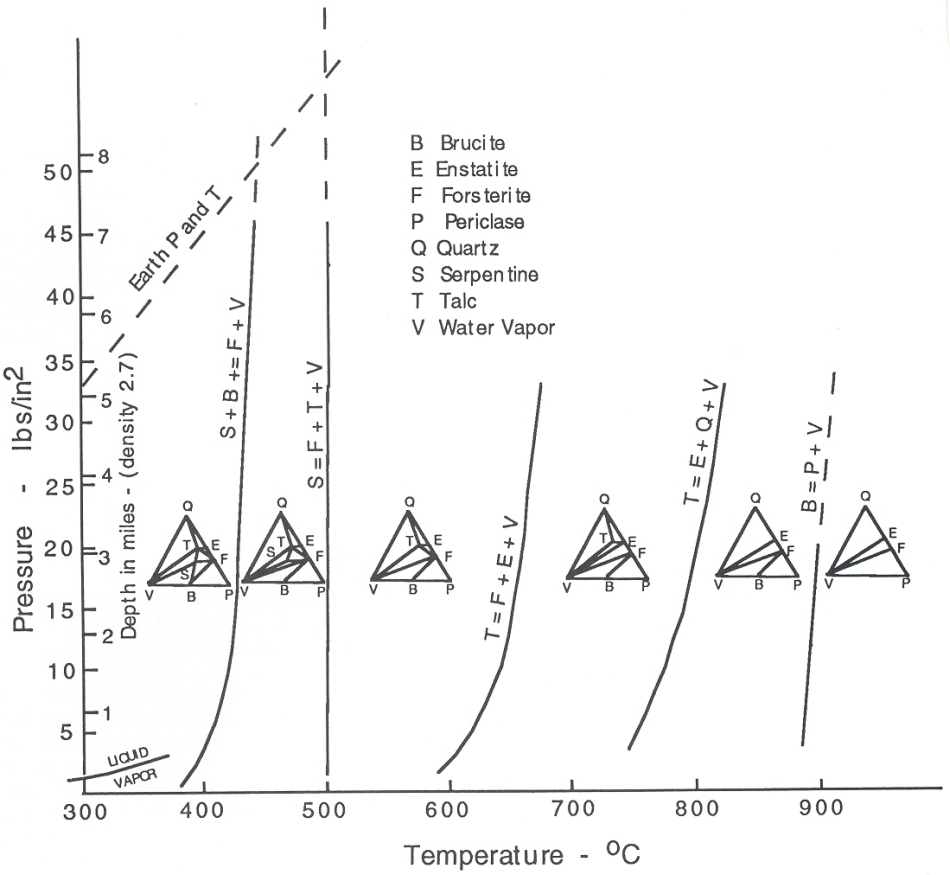

Fig. 1-3. Phase diagram constructed by Bowen and Tuttle (1949), summarizing their experimental work in the system MgO-SiO_2-H_2O. (After Bowen and Tuttle, 1949.)

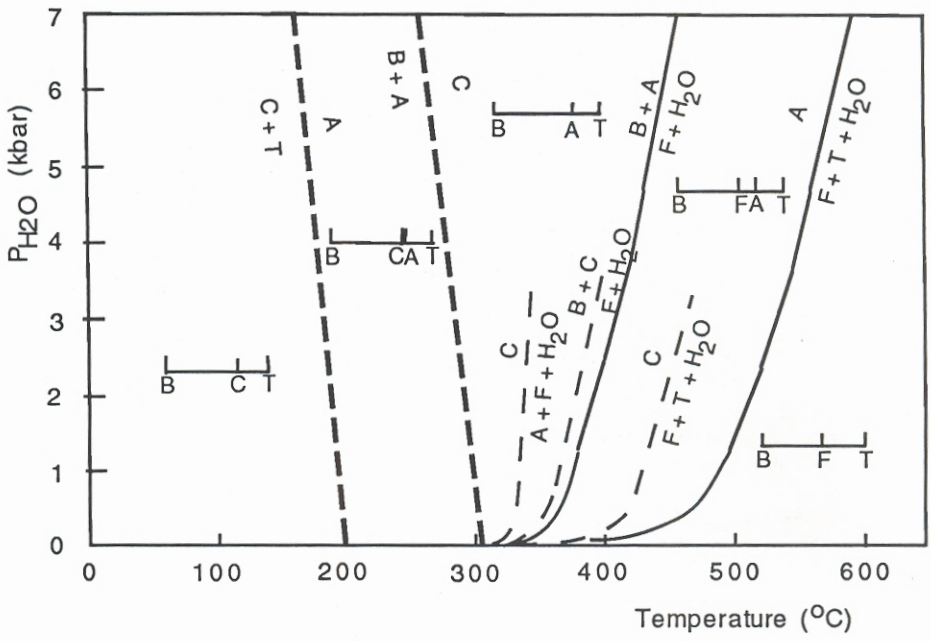

Fig. 1-7. Phase diagram constructed by Evans et al. (1976), which represents the first phase diagram for the serpentine system consistent with available field and analytical data. (Reprinted by permission of Stäubli Verlag AG.)

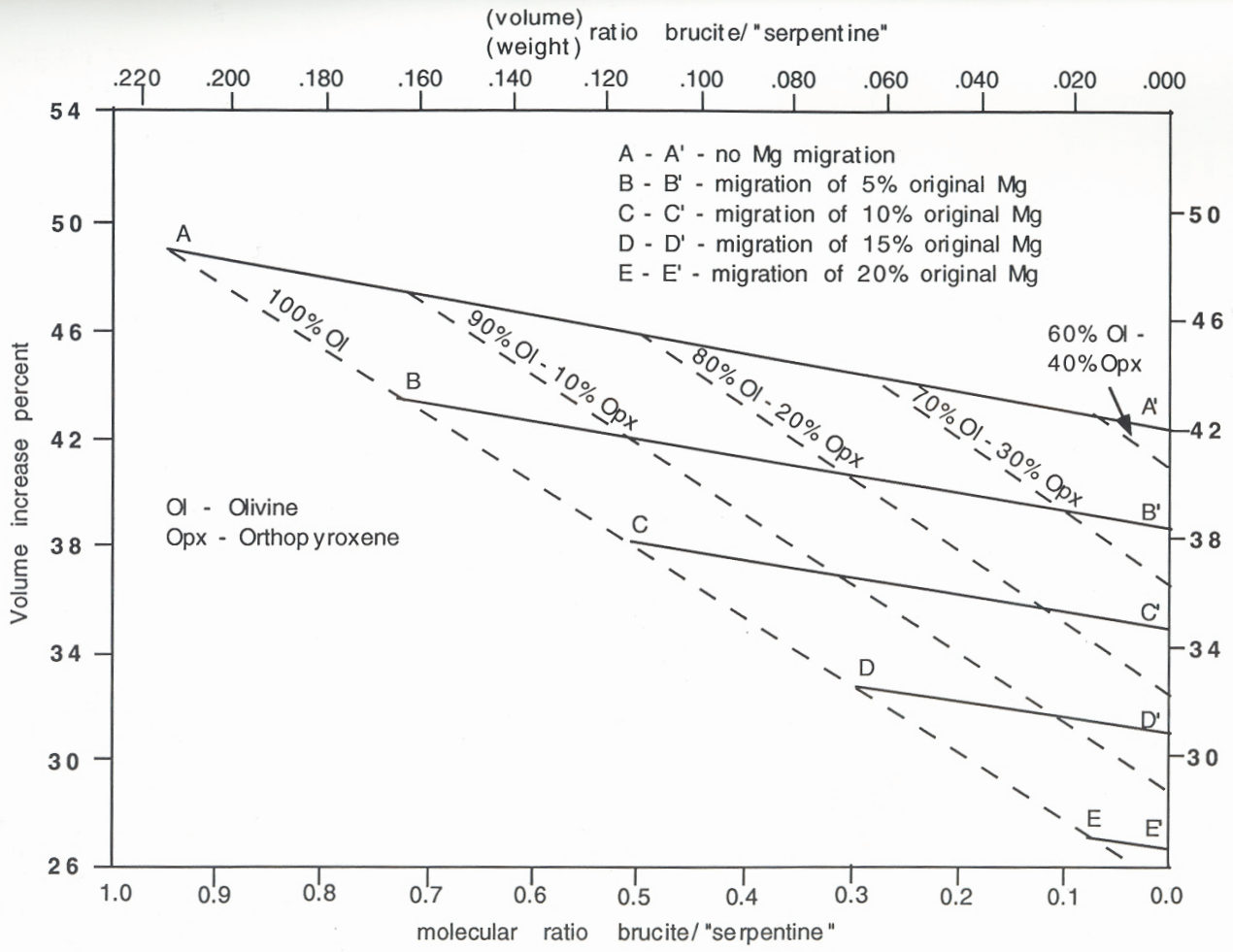

Fig. 1-9. Nomogram for calculating the percent increase in volume accompanying serpentinization based on the measured modes of both unaltered and serpentinized peridotite. (After Hostetler, P.B., et al., 1966. Brucite in alpine serpentinites. *Am. Mineral.* **51,** 75–98, Fig. 2, copyright by the Mineralogical Society of America.)

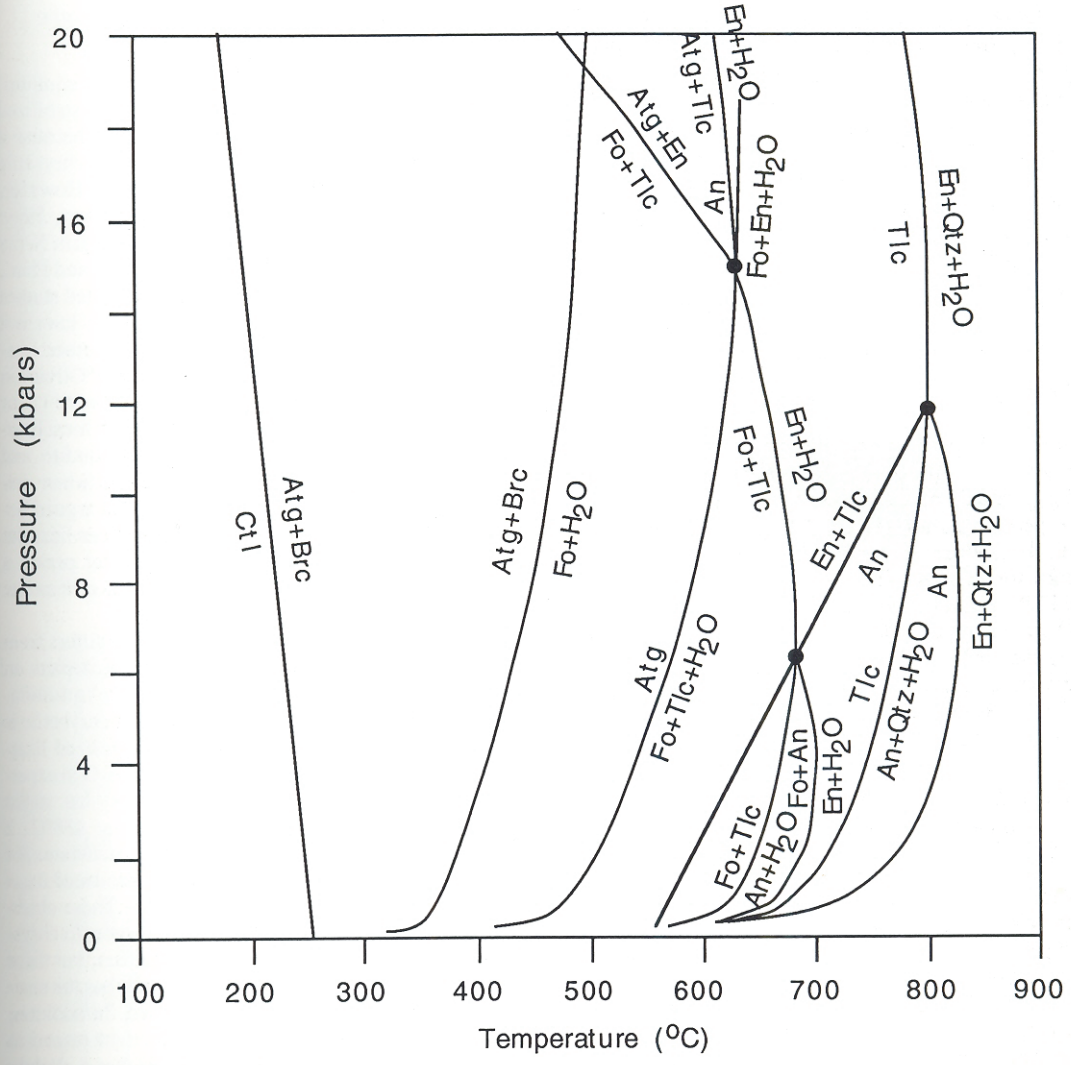

Fig. 2-3. P-T relations among the phases chrysotile (Ctl), antigorite (Atg), brucite (Brc), forsterite (Fo), talc (Tlc), enstatite (En), anthophyllite (An), quartz (Qtz), and H_2O, in the system $MgO\text{-}SiO_2\text{-}H_2O$. The equilibrium Fo + Tlc = Atg + En and the part of the equilibrium En + Tlc = An located below the invariant point are not appropriate for $P(H_2O) \approx P_{total}$. (After Berman et al., 1986. J. Petrol., by permission of Oxford University Press.)

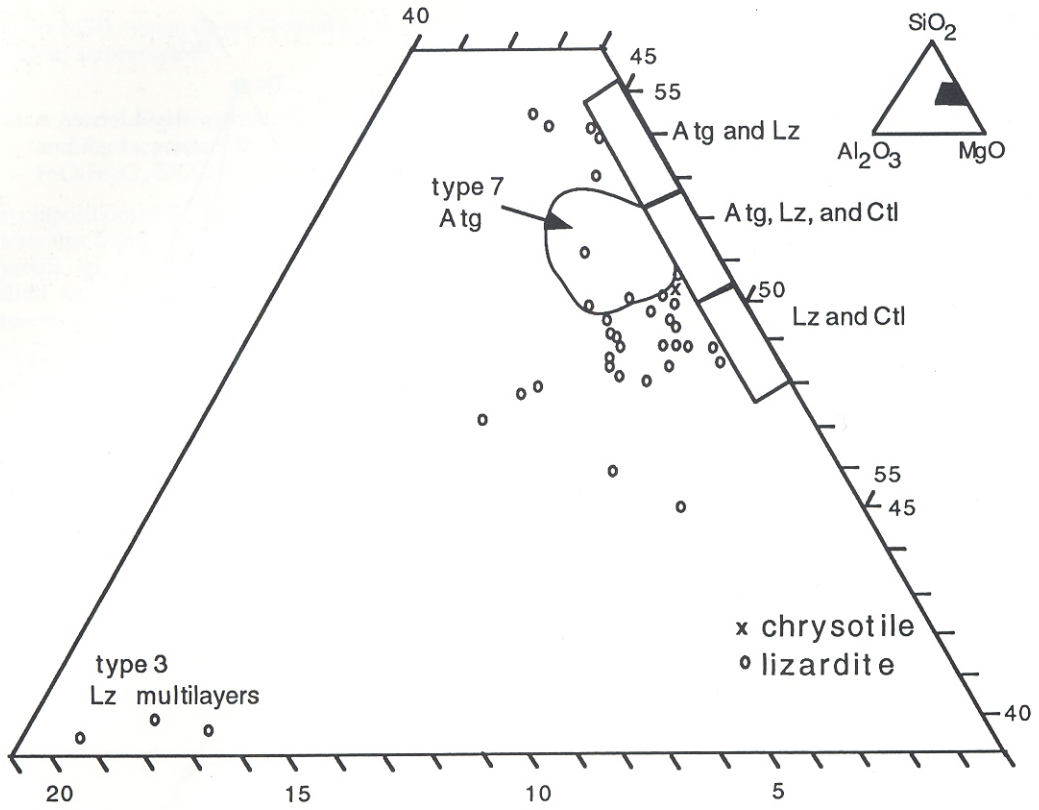

Fig. 2-9. Renormalized SiO_2-Al_2O_3-MgO values of serpentine minerals obtained by electron microprobe. Boxes contain high concentrations of analyses (144 out of 185 analyses). Types of serpentines are given in Table 2-2. (Adapted from Wicks and Plant, 1979. Reprinted by permission.)

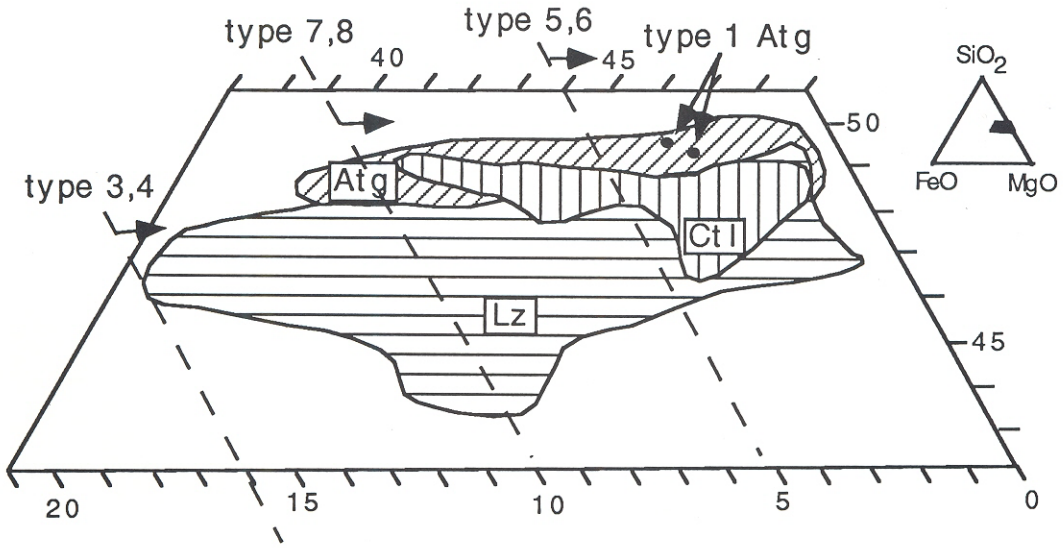

Fig. 2-10. Renormalized SiO_2-FeO-MgO values of serpentine minerals obtained by electron microprobe. Total Fe is represented as FeO. Types of serpentinites are given in Table 2-2. (Adapted from Wicks and Plant, 1979. Reprinted by permission.)